Biophysical Journal Volume 68 March 1995 1170–1176

Cross-Linking of CD4 in a TCR/CD3-Juxtaposed Inhibitory State: A pFRET Study

Gábor Szabó Jr.,*‡ James L. Weaver,‡ P. Scott Pine,‡ Patricia E. Rao,§ and Adorjan Aszalos‡

*Department of Biophysics, University Medical School of Debrecen, 4012 Hungary; ‡Center for Drug Evaluation and Research, Food and Drug Administration, Washington, D. C. 20204; and §Ortho Diagnostic Systems, Inc., Raritan, New Jersey, 08869, USA

ABSTRACT Instances when T cell activation via the T cell receptor/CD3 complex is suppressed by anti-CD4 Abs are generally attributed either to the topological separation of CD4-p56^{lck} from CD3, or their improper apposition. Photobleaching fluorescence resonance energy transfer measurements permitted direct analysis of these alternatives on human peripheral blood lymphocytes. Distinction between changes of relative antigen densities or positioning was made possible by simultaneously recording donor and acceptor fluorescence in the energy transfer experiment performed on homogeneous populations of flow-sorted cells. We show here that CD4 stays in the molecular vicinity of CD3, while anti-CD3 stimulation is suppressed by anti-CD4 or cross-linked HIV gp120. Our data suggest that cross-linking of CD4 through particular epitopes is capable of inhibiting activation driven by Abs binding to specific sites on CD3 without major topological sequestration of the Ags, in such a way that additional positive signals will also be affected. Thus, these and other related cases of negative signaling via CD4 may be interpreted in terms of functional uncoupling rather than a wide physical separation of CD4 from the T cell receptor-CD3 complex.

INTRODUCTION

T cell activation evoked via the T cell receptor/CD3 (TCR/CD3) complex is normally potentiated by co-engagement of CD4 mediated by major histocompatibility complex (MHC) class II molecules of the Ag-presenting cell (Dianzani et al., 1992; Haque et al., 1987; Mittler et al., 1989; Rojo et al., 1989; Saizawa et al., 1987; Kupfer et al., 1987). CD4 appears to deliver an activated protein tyrosine kinase p56^{lck}, noncovalently attached to its cytoplasmic end, to TCR/CD3 upon their co-aggregation (Abraham et al., 1991; Veillette et al., 1988; Rudd et al., 1988; Straus and Weiss, 1992; Collins et al., 1992; Glaichenhaus et al., 1991). Anti-CD4 Abs (Janeway, 1989; Newell et al., 1990; Bank and Chess, 1985), even fragments involved in antigen binding (Fab; Haque et al., 1987) and peptide fragments of the CD4 molecule (McDonnell et al., 1992), have been described as exhibiting a negative effect on T helper cell activation elicited by certain anti-TCR/CD3 Abs or Ag. At an early stage of activation, its suppression by CD4 ligation may be explained by (1) steric separation (Newell et al., 1990; Nel et al., 1990; Haughn et al., 1992) of the TCR/CD3 complex from CD4; or (2) specific conformational-topological constraints (Haughn et al., 1992) imposed on the TCR/CD3/CD4 complex. This latter condition either (2a) prevents the development of an active TCR/CD3 conformation (Rojo and Janeway, 1988) elicited normally by MHC, or (2b) may represent a negative signal (Newell et al., 1990; Bank and Chess, 1985) that counteracts activation via productively engaged receptors of the same cell (or same multi-receptor complex). The special case of model 1, when minimal spatial separation would prevent direct contact of the Ags (without their large-scale sequestration as visualized in cocapping experiments), appears functionally equivalent to model 2. Up until now, it has not been possible to distinguish between broad physical sequestration and functional uncoupling of TCR/CD3 and CD4 or steric distortion of the complex.

A highly sensitive version (Szabó et al., 1992a; see Materials and Methods for recent modifications) of the photobleaching fluorescence resonance energy transfer method (pFRET; Jovin and Arndt-Jovin, 1989)) permitted the measurement of molecular distances between receptor-bound Abs, and enabled us to distinguish between the above possibilities on peripheral blood leukocytes (PBL). FRET techniques are applied to measure the efficiency (E) of the transfer of excitation energy from an excited donor to a proximal acceptor, according to the $E = R_0^6/(R_0^6 + R^6)$ equation, used as a molecular ruler for the donor-acceptor distance (with R_0 = 10 nm in our case; see Szabó et al., 1992a). We showed that phycoerythrin (PE, attached to antibody), is a very efficient acceptor when fluorescein is the donor (conjugated with another antibody as its isothiocyanate, FITC). The photobleaching version of this technique is based on the finding (Jovin and Arndt-Jovin, 1989) that the kinetics of photobleaching are slower when a spectrally adequate energy acceptor is in close proximity to the donor. We have recently further developed this approach to carry out pFRET measurements in a laser microscope system (Szabó et al., 1992a). The utility of the technique in detecting intramolecular conformational changes of CD4 (Szabó et al., 1992b), and the Leu8 antigen (Szabó et al., 1993) on human peripheral blood T cells has been demonstrated.

In the present work we approximate the degree and pattern of redistribution of cell surface molecules (CD4, TCR, CD3) upon treatment with various antibodies, used for treatment and as fluorescent label at the same time, demonstrating the

Received for publication 8 June 1994 and in final form 18 November 1994.

Address reprint requests to Dr. Gábor Szabó Jr., Department of Biophysics, University Medical School of Debrecen, 4012 Debrecen, Nagyerdei krt 98, Hungary. Tel.: 36-52-412623; Fax: 36-52-412623; E-mail: szabog@jaguar.dote.hu.

0006-3495/95/03/1170/07 $2.00

method's utility for the assessment of intermolecular distances on human PBL. Since E is measured on the donor side in pFRET, its value is a function of both the (inherently large) cell-to-cell variations of the donor/acceptor ratio, and of the changing topology (with antigen densities maintained). To distinguish between these alternatives we measured both the donor and acceptor fluorescence, performing pFRET on homogeneous samples of flow-sorted cells.

MATERIALS AND METHODS

Cells

PBL of healthy donors were prepared from the interface of Histopaque-1077 (Sigma Chem. Co., St. Louis, MO, USA) gradients. ^{3}H-thymidine incorporation was measured using 0.5 μCi/microwell 86 Ci/mmol isotope (Amersham, UK) in 4-h pulses, after 3 days of culturing in RPMI 1640 + 10% FCS, glutamine, penicillin, and streptomycin, and monoclonal Abs (mAbs). The anti-CD3 Abs Leu4, and wt31 (product name: anti-TCRα/β) were from Becton Dickinson (Mountain View, CA), UCHT1 was from DAKO Corp. (Carpinteria, CA). OKT3 (anti-CD3), as well as the TCRα/β-specific OKT3a were from Ortho Diagnostic Systems, Inc. (Raritan, NJ). The following CD4-specific antibodies and ligands were used: Leu3a (Becton Dickinson), OKT4a, and OKT4 (Ortho Diagnostic Systems), Sim.4 (AIDS Research and Reference Reagent Program NIAID, NIH, Bethesda, MD); Abs 463 and 818, recombinant gp120-HSV chimeric protein, and anti-HSV Ab 5B6 were from Genentech, Inc. (South San Francisco, CA). For immunostaining of cells, usually 100 ng of the Abs from Becton Dickinson and DAKO, or 1 μg of OKT4E or OKT3a were used, except where noted. The FITC/protein ratios of all the Abs used were between 4 and 5. Fluorochrome-conjugated Abs were added to 1×10^6 cells in 0.1 ml phosphate-buffered saline (PBS, pH 7.4) and incubated for 30 min on ice. In some experiments (Table 1), fluorochrome-conjugated Abs were added to PBL in complete medium at the usual cell concentration of 1×10^6 cells/ml and allowed to act on the cells (Abs used as treatment) as well as label them, for 30 min. The cells were washed twice with ice-cold PBS and fixed for 1 h in 1% paraformaldehyde (in PBS), followed by flow-cytometric (FACScan (Becton Dickinson, used with the "Research software", or software version "Consort 30") or Coulter Corp. (Hialeah, FL) Elite V) analysis and separation (Coulter) from ice-cooled tubes onto slides, for immediate pFRET analysis in the ACAS 570 system (see below).

pFRET measurements

Photobleaching data collection for pFRET (Jovin and Arndt-Jovin, 1989, Szabó et al., 1992a, b, 1993)) was performed basically as described (see Szabó et al., 1992a) with several modifications, however, as pointed out below, on an ACAS 570 stage scanning laser (fluorescent) microscope (Meridian Instruments, Okemos, MI), using an Olympus 100× oil immersion objective lens (Olympus Corp. San Francisco, CA). The cells were positioned in the center of a laser illumination spot expanded by a beam diffuser to a size of 30 μm in diameter. The argon laser was set for 1000 mW at 488 nm. Fluorescence intensity data, from the FITC as well as from the PE channel, were collected using the "point scan" mode of the ACAS Kinetics Analysis software (version 2.0h). FITC bleaching curve data were extracted from the 2000 points of the ACAS *.kpt data file, smoothed and fitted to a double exponential equation. The fitted data set of 100 data points and the parameters of the fitted equation were imported into a spreadsheet program (Quattro Pro 3.0, Borland Inc., Scotts Valley, CA).

The fixed donor-only and donor-+-acceptor (D, D + A)-labeled cells were flow sorted from identical FL1 (FITC) and FL2 (PE) windows for the analysis of donor photobleaching kinetics. E was measured using the

$$E = 1 - \frac{T_{avg}}{T'_{avg}}$$

TABLE 1 Ab-Ab distance measurements by pFRET, with samples prepared by flow sorting

Donor (expt. no.)	Acceptor	Treatment	E' or $\Delta E'$ (expts. 5–7)	E
OKT3a (1)	Leu3a		15.2 ± 2.2	17.5
OKT3a (1)	Leu3a	wt31	23.0 ± 2.0	23.0
OKT3a (2)	Leu3a		10.3 ± 1.2	10.3
OKT3a (2)	Leu3a	wt31	30.8 ± 0.8	33.9
OKT3a (2)	Leu3a	wt31 + Leu3a	31.3 ± 1.0	35.2
OKT3a (2)	Leu3a	Leu4	31.6 ± 0.8	36.1
OKT3a (2)	Leu3a	Leu4 + Leu3a	30.6 ± 0.9	35.9
OKT3a (1–4)	Leu3a		9.0 ± 2.4	
OKT4 (5–7)	Leu4	gp120 + X	3.5 ± 0.4	
Leu3a (8)	UCHT1		6.0 ± 1.2	
Leu3a (8)	UCHT1	UCHT1	8.9 ± 1.2	
Leu3a (8)	UCHT1	UCHT1 + Leu3a	15.5 ± 1.1	
Leu3a (8)	Leu4	Leu4	20.8 ± 1.3	
Leu3a (8)	Leu4	Leu4 + Leu3a	31.5 ± 1.1	
OKT3a (9)	CD45RO		−0.5 ± 2.4	
wt31 (10)	Leu3a	wt31 + Leu3a	17.9 ± 1.7	17.9
Leu4 (10)	Leu3a	Leu4 + Leu3a	9.4 ± 1.1	10.4
wt31 (11)	Leu3a	wt31 + Leu3a	14.4 ± 1.5	14.4
Leu4 (11)	Leu3a	Leu4 + Leu3a	8.4 ± 1.1	9.2
wt31 (12)	Leu3a	wt31 + Leu3a	12.2 ± 1.2	12.2
Leu4 (12)	Leu3a	Leu4 + Leu3a	8.6 ± 1.0	9.9
OKT4E (13)	UCHT1	UCHT1	8.8 ± 2.9	
OKT4E (13)	Leu4	Leu4	15.7 ± 2.2	

Changes of the E' observed energy transfer efficiency values are directly indicative of topological changes in the case of experiments 8 and 13; the (normalized) E values are informative in the other experiments (see Materials and Methods). Fluorescence labeling of 10^6 PBL was performed either in PBS at 0°C, or at 37°C in complete medium for 30 mins when these Abs also served for a treatment (e.g., with Leu3a-PE in experiment 2). Leu4 doses producing approximately wt31-equivalent fluorescence were applied in the case of experiments 10–12. SE was calculated for $n = 49$ (applying the error propagation function on the primary SE values of T_{avg}), or between batches (experiments 1–4 and 5–7). $\Delta E'$ = change of E' (experiments 5–7).

relationship (with T_{avg} and T'_{avg} representing the average (Szabó et al., 1992a) half-lives of the donors upon bleaching in the absence and in the presence of a proximal A, respectively). The subscript refers to the fact that double-exponential fluorescence-decay kinetics are observed, and the average of the two time constants weighted by the corresponding amplitudes provides T_{avg} (see Szabó et al., 1992a). Depletion of the excited states due to FRET is reflected in the prolongation of the T'_{avg} value (relative to T_{avg}), making the calculation of E possible, according to the above equation. The FL1 and FL2 decay were registered simultaneously and the

$$r' = \frac{FL1_{integral}}{FL2_{initial}}$$

relative D/A fluorescence (cell labeling) ratios were calculated for each curve (cell), after subtracting the post-bleach (background) levels of green and red fluorescence. (The fluorescein/protein ratios for each FITC conjugate used were between 4 and 5, based on batch-specific data, a courtesy of Becton Dickinson.) Their r average for the 50 (D + A)-labeled cells was used to obtain E (true energy transfer efficiency) from E' (efficiency calculated directly from the observed decay time constants), in the normalization procedure discussed below. The overestimation of r (just as its high true (real) value) incurs low transfer efficiencies, depriving the method of its sensitivity, while its underestimation would exaggerate small differences in E. The calculated r values themselves were normalized to $r = 1$. A value of $r = 1$ was assumed for the E determinations within each data set where E measured and calculated for the CD3-to-CD4 transfer rendered E values

similar to those measured in the opposite direction (from CD3 to CD4). Relative r values were calculated for the rest of the data within that set. E is independent from the direction of transfer at $r = 1$, whereas it strongly depends on the direction of transfer at r values different from 1, as illustrated below:

$$r = 1 : \text{CD3 CD4 CD3–CD4}$$

$$r > 1 \quad \text{or} \quad r < 1 : \text{CD3 CD3–CD4} \quad \text{or} \quad \text{CD4 CD3–CD4}$$

(Complete independence or specific association of the Ags involved are the two possible alternatives considered here; using FL2 (initial intensity-background) as a measure of A labeling of the cells carries a minor error due to energy transfer itself.)

Assuming a 1:1, specific D-A association that involves most of the available partner molecules present at the smaller (limiting) concentration, the following two cases are considered. 1) When A ≥ D (and the surplus A is outside FRET distance from D), T'_{avg} (and E) will be invariant to r. Thus, in the case of an anti-CD4 donor and anti-TCR/CD3 acceptor, E' will indicate the D-A proximity within these complexes. 2) If D > A (i.e., there is a population of free Ds; anti-TCR/CD3 donor and anti-CD4 acceptor), T'_{obs} (observed, apparent T'_{avg}) and E', respectively, will be sensitive to D/A = r, because

$$E' = 1 - \frac{T_{avg}}{T'_{obs}}$$

and

$$T'_{obs} = (A * T'_{avg} + (D - A) * T_{avg})/D$$

with T'_{obs} expressed as the average of decay time constants weighted by the complexed and uncomplexed Ds, according to their respective ratios. From the above, E within the D-A complexes presents (at $r \geq 1$):

$$E = r * \frac{E'}{1 + (r - 1) * E'}$$

In order to assess the degree and changes of intimacy between D and A, the (corrected) E values are to be compared in case 2 (anti-TCR/CD3 D, anti-CD4 A), when differences in D/A strongly influence E, even without changes in D-to-A proximity. The (observed) E' will be indicative of this relationship when 1 seems to be the case (anti-CD4 D, anti-TCR/CD3 A), i.e., in the absence of uncomplexed (solitary) D. Saturation of the available D and A sites with Abs is assumed in the above model.

To further minimize biological variation, cells from samples to be compared were sorted from identical FL1 and FL2 windows for immediate pFRET analysis. In addition, the cell-to-cell distribution of the FL1 integral values, as well as that of the T_{avg} and T'_{obs}, were always evaluated in correlation with various other parameters (time of data collection, FL2, etc.) on the worksheet program (Quattro) to recognize possible cell-to-cell heterogeneities and instrument instability. The experiments had been devised to compare parallel samples of the same batch of cells labeled and measured in alternating sequence on the same day. In our system, comparison of up to four sample pairs (D- and (D + A)-labeled cells) was made possible on a daily basis.

RESULTS

Epitope-specific inhibition of anti-CD3-stimulation of PBL by CD4 cross-linking

Anti-CD3-induced activation of PBL was strongly inhibited by CD4 ligation, as shown in Fig. 2; see Fig. 1 for illustration of the epitope specificities of the mAbs discussed below. The Leu3a Ab (IgG_1), specific for a CD4 epitope overlapping the HIV gp120 binding site (Sattentau et al., 1986) suppressed wt31 (anti-CD3, IgG_1) stimulation dramatically. This inhibition was dose-dependent (Fig. 2 *A*). The effect of CD4 ligation on Leu4 (also anti-CD3, IgG_1) stimulation was much

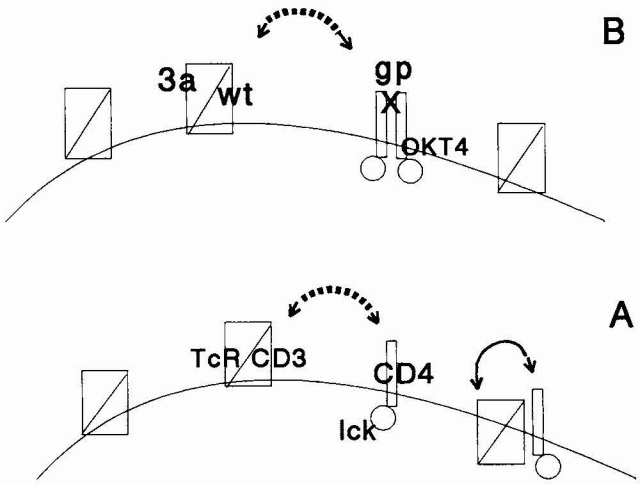

FIGURE 1 Schematic representation of the T helper cell surface. wt, overlapping binding sites of wt31, Leu4, and UCHT1; gp, overlapping binding sites of HIV gp120, the Leu3a, OKT4a and Sim.4 mAbs; 3a, OKT3a specific for TCRα/β; OKT4, membrane proximal OKT4 epitope. Arrows connect juxtaposed or distant TCR/CD3 and CD4 receptors, on the scale of fluorescence resonance energy transfer. The rectangular symbols represent receptor doublets assumed to be present to account for their capping by mAbs. (*A*) Some CD4s are associated with TCR/CD3 complex, which is a substrate for the lck kinase attached to CD4. (*B*) CD4s are sequestered by their cross-linking.

less marked, or on some batches of PBL, even stimulatory (see Fig. 2 *A* and Table 2).

Fig. 2 *B* demonstrates that treatment of PBL with gp120 + anti-gp120 had an effect identical with that of Leu3a, or the competing (Sattentau et al., 1986) OKT4a and Sim.4 (Table 2). At the same time, gp120 alone decreased activation to a lesser extent, probably due to the CD4 conformational change shown to result from binding of gp120 (Szabó et al., 1992b). The requirement for cross-linking in the case of gp120 treatment to completely suppress wt31-evoked stimulation suggested that cross-linking, and not just the ligation of CD4, was necessary for this effect. However, several bivalent anti-CD4 Abs (e.g., OKT4; see Table 2) failed to affect stimulation in a similar fashion. (We could directly demonstrate the cross-linking effect of OKT4, using OKT4-FITC and OKT4-PE as the D-A pairs, data not shown.) Thus, cross-linking of CD4 in an epitope-specific manner was responsible for suppression.

On the other hand, the specificity of the anti-TCR/CD3 Ab determined the outcome of anti-CD4 co-treatment. Stimulation evoked by OKT3a (anti-TCRα/β) was not inhibited (see Table 2). Activation via anti-CD3 Abs OKT3 or Leu4 was only mildly inhibited or even augmented, whereas activation by wt31 and UCHT1 was inhibited by 75–95%, although Leu4, OKT3, UCHT1, and wt31 appear to recognize overlapping epitopes formed by the ϵ plus γ or δ chain (Salmeron et al., 1991). Thus, stimulation of PBL by mAbs, competing for mutually exclusive binding sites on CD3, was differentially affected by CD4 cross-linking. The extent of inhibition did not correlate with the level of stimulation, which showed great PBL batch-to-batch variability for both

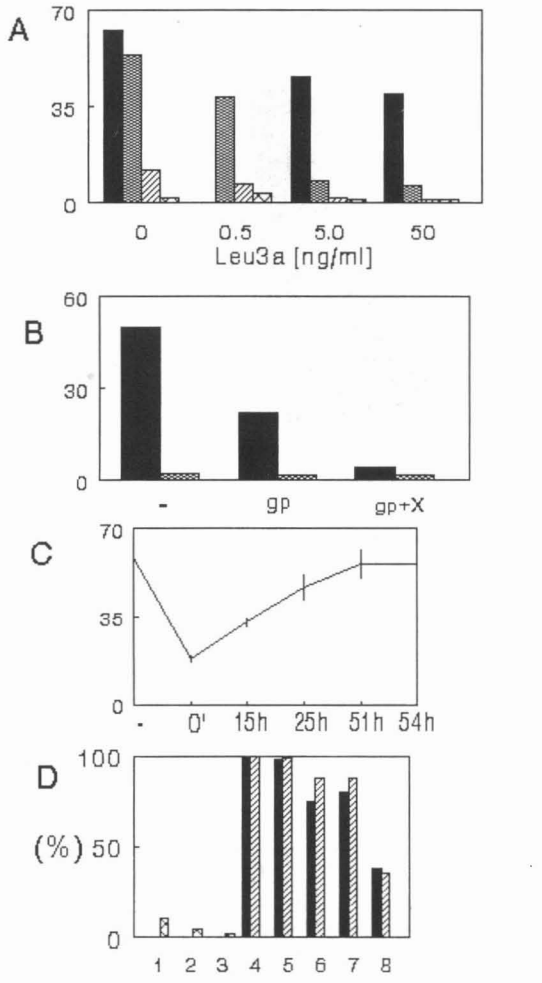

FIGURE 2 Effect of CD4 ligands on anti-TCR/CD3-induced T cell activation in human PBL cultures. Cells were harvested after 3 days of incubation with the ligands, with ^{3}H-thymidine added in the last 4 h. *y* axis: dpm in thousands. (*A*) PBL stimulated with anti-CD3 Abs in the absence or presence of Leu3a (used at the concentrations shown). Leu4 (5 ng/ml): black bars; wt31 (applied at 50, 5, and 0.5 ng/ml concentration): gray, hatched, and cross-hatched bars, respectively. (*B*) PBL stimulated with wt31 (black bars; Ab used at a concentration of 25 ng/ml), in the presence of gp120-HSV alone (gp; applied at 1 μg/ml), together with anti-HSV Ab 5B6 (gp + *X*; see Banda et al., 1992) used at 5 μg/ml) or without these additions (−). In parallel experiments Leu3a was also included during incubation (gray bars; Leu3a used at 50 ng/ml). (*C*) PBL stimulated with wt31 (25 ng/ml); with Leu3a (50 ng/ml) added after wt31 at the times indicated. SE was as indicated by the bars, with similar values (not shown) in the other panels. (*D*) PBL were first incubated (1 h at 37°C, in complete medium) with the Abs indicated (*; 12.5 ng/ml); then the second inducer Ab‡ was also added (OKT3a (black bars) or OKT3 (hatched bars), both used at 12.5 ng/ml) as shown in the tabulation below. Thymidine incorporation was measured after 3 days of incubation with the second Ab (means of three experiments shown). 100% = 160,000 dpm.

	1	2	3	4	5	6	7	8
wt31	+*	+*	−	−	+*	+*	+‡	+*
Leu3a	−	+*	−	−	−	−	−	+*
OKT3a/OKT3	−	−	−	+*	+*	+‡	+*	+‡

wt31 and Leu4 (compare, e.g., Fig. 2, *A–C* with *D*). Activation appears to be blocked by Leu3a at an early stage (Fig. 2 *C*); accordingly, the early $[Ca_i]^{2+}$ increment evoked by

TABLE 2 Suppression of anti-CD3-induced T cell activation by anti-CD4 Abs of different epitope specificities (activation measured by thymidine incorporation; see Materials and Methods)

Stimulation			Treatment	Change
Leu4	wt31	Other		%
+			Leu3a	+25.0
	+		Leu3a	−85.3
+			OKT4	−36.0
	+		OKT4	+19.6
+			463	+17.3
	+		463	+38.8
+			818	+16.3
	+		818	+19.7
	+		Sim.4	−74.7
	+		OKT4a	−80.0
		OKT3a	Leu3a	+17.0
		OKT3	Leu3a	−8.0
		UCHT1	Leu3a	−86.0

(cross-linked) wt31 was largely diminished by gp120 + anti-gp120 or OKT4a (data not shown).

Negative signaling (see case 2b above) may be involved, given that stimulation by OKT3a or OKT3 was prevented by wt31 plus Leu3a pretreatment (Fig. 2 *D*). This negative effect was not due to a significantly decreased binding of the secondary stimulating agents since labeling with the second step Abs was not affected by incubations in the first step, as judged by flow cytometry. This negative effect was abolished when the low-affinity wt31 Ab was washed off the cells after the first incubation step (data not shown). These data imply that the suppressive effect is generated at an early step of activation and involves some kind of interaction between CD3 and CD4.

pFRET analysis of TCR/CD3-CD4 proximity relationships

Fig. 1 illustrates two antithetical cell surface topological arrangements: with CD4 staying in the molecular vicinity of TCR/CD3 (Fig. 1 *A*), or becoming sequestered (Fig. 1 *B*). (Association of CD4 with TCR/CD3 is assumed to occur upon activation; see Dianzani et al., 1992; Haque et al., 1987; Mittler et al., 1989; Rojo et al., 1989; Saizawa et al., 1987; Kupfer et al., 1987). Broad spatial sequestration of cross-linked CD4 away from TCR/CD3 would be reflected in the absence of fluorescence energy transfer between anti-TCR/CD3 Abs and anti-CD4 Abs. In contrast, a detectable level of energy transfer would be compatible with model 2 above, or the special case of model 1 when a small separation would prevent direct contact of the Ags without their extensive sequestration. Performing pFRET (Jovin and Arndt-Jovin, 1989) adapted to a laser scanning image analyzer system (Szabó et al., 1992a), using FITC-labeled mAb as the donor (D) and PE-tagged Ab as the acceptor (A), allowed us to address this question on PBL. Because the energy transfer efficiency also depends upon the D/A ratio, we compared samples flow sorted from identical sort windows and also

normalized within the compared set of samples for actual labeling differences (corrected E values; see Materials and Methods). It is to be emphasized that fluorescence labeling was part of the treatment and cell stimulation schedule (see Materials and Methods and Table 1 legend), ensuring that the observed topology was biologically relevant. The high E values between OKT3a-FITC and Leu3a-PE before stimulation (Table 1, experiments 1–4) implied significant CD4-TCR/CD3 association on resting cells, supporting the validity of recent coprecipitation and affinity chromatography data (see Suzuki et al., 1992; for conflicting data see Gallagher et al., 1989). A further increase in E with activation confirmed the current dogma on the association of CD4 and TCR/CD3 becoming more complete upon stimulation (Mittler et al., 1989; Rojo et al., 1989; Kupfer et al., 1987). Moreover, E between CD4 and TCR/CD3 was maintained at its high post-stimulation level in the presence of Leu3a-PE (applied both as A and for treatment), strongly arguing against model 1. The flow-cytometric FL1/FL2 distribution of wt31-FITC/Leu3a-PE (specific for CD3 and CD4, respectively) stained PBL, with the subpopulation sorted for pFRET marked, is shown in Fig. 3 (upper panel). Monitoring FL2, as well as FL1 in the bleaching experiment (see also Materials and Methods) allowed us to view the data in a scattergram representation, as in Fig. 3 (lower panel). The prolonged T_{avg} values of most FL2-positive cells agree with a significant level of CD3-CD4 energy transfer that shows no obvious population heterogeneity. Cross-linking by Leu3a (experiment 8) or through gp120 (experiments 5–7) even increased CD4-CD3 juxtaposition when E′ was measured, in the opposite direction (from CD4 to CD3) (experiments 5–8) and between the particular Abs also used in the stimulation experiment (experiment 8). In contrast, there was no energy transfer from OKT3a toward CD45RO-PE (experiment 9), which was in accordance with flow-cytometric FRET data (Mittler et al., 1991).

Experiments 10–12 of Table 1 support the possibility that the proper steric arrangement within the TCR/CD3/CD4 complex might be hindered by CD4 cross-linking, given that E and E′ between wt31 and Leu3a was greater than between Leu4 and Leu3a, suggesting a higher degree of proximity between the antagonizing Abs. In contrast (experiment 13), the OKT4E Ab (binding to an epitope opposite to the gp120 site (see Szabó et al., 1992b)) appears to be much closer to Leu4 than to UCHT1 (wt31-like in terms of Leu3a-sensitivity, see Table 2), suggesting a position-sensitive steric arrangement of the Ags. Therefore, the Ab wt31 (or UCHT1) is either in a more intimate steric relationship with the suppressor Ab than is Leu4, or wt31 is preferentially bound to CD3/TCR molecules more intimately involved with CD4.

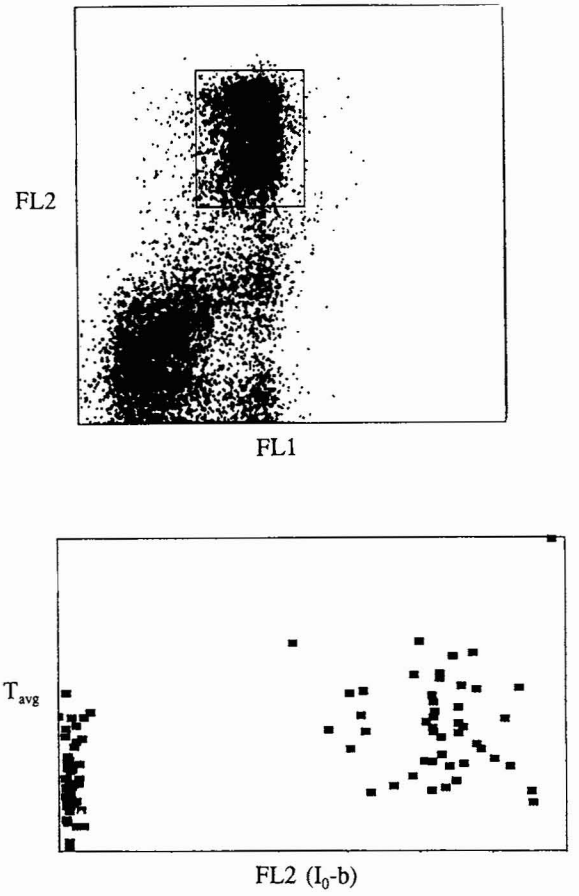

FIGURE 3 (*Upper panel*) Flow-cytometric dot plot of PBL labeled with wt31-FITC and Leu3a-PE (CD3, FL1 and CD4, FL2, respectively; *X-Y* scale: log-log). Window shows the subpopulation of double-positive cells selected for flow-sorting. Lower panel. Dot plot representation of pFRET data. T_{avg} is plotted as a function of FL2, combining the photobleaching data obtained from D-only (left group of filled squares) and (D + A)-labeled cells (right group of squares). Linear *X-Y* scale (arbitrary units).

DISCUSSION

The high CD4-TCR/CD3 E (and E') values (close to the maximal intramolecular E values measured in this system (Szabó et al., 1992a, b) in the presence of CD4 cross-linking are incongruous in the context of the currently most-favored interpretation (see Julius et al., 1993 for review) that an Ab-evoked spatial sequestration of CD4 is responsible for this example of immune suppression. The data favor a model (2b, above) where an improper apposition of CD4 with TCR/CD3, forced by the binding of both wt31 and Leu3a distorts the whole complex (or agglomerate of complexes), and impairs positive signaling by additional anti-CD3 Abs. Thus, the cases of negative signaling via CD4 (Julius et al., 1993) may be due to functional uncoupling rather than physical separation of CD4 + $p56^{lck}$ from TCR/CD3. The fact that CD4 and the CD3 ϵ chain can be coprecipitated by anti-CD4 Abs (i.e., anti-CD4 does not induce the in vitro dissociation of the complex; see Burgess et al., 1991) supports our findings.

The anti-CD4 and anti-CD3 Abs could sterically prevent the approximation and direct contact of the Ags by their direct bumping into each other, indicated by the significant energy transfer between the Abs. In this case, the Ag-Ag separation should be within a range of ~10–20 nm, preventing their direct contact. This situation is functionally

equivalent to the steric distortion of the complex (with CD4 and TCR/CD3 juxtaposed) when CD4-p56^{lck} becomes disengaged from TCR/CD3. Beyond these strictly mechanistic considerations, it is also possible that the proximity relationships correlate with the tightness of CD4-p56^{lck} anchorage, and thus affect activation indirectly.

The fact that suppression is released by washing off of wt31 (data discussed above) raises the possibility that the inhibitory effect involves a negative signal generated by the wt31 + Leu3a-distorted TCR/CD3/CD4 complex. Since the different domains of lck have distinct functions that may independently contribute to T cell activation (Xu and Littman, 1993), such a scenario is not at variance with the context of prevailing biochemical evidence. The versatility of possible interactions through the kinase SH2 and SH3 domains and the disparate roles of the possible phosphorylation sites generate a complexity compatible with alternate induction pathways, including negative signaling (see Xu and Littman, 1993; Luo and Sefton, 1990; Burgess et al., 1991). Our results suggest that the interaction of TCR/CD3 components with CD4 must be sterically coordinated (in vivo by MHC class II Ags) for activation signaling (in line with the recent molecular model described in Langedijk et al., 1993) and also provide a mechanistic framework for the possibility (Banda et al., 1992; Mittler and Hoffmann, 1989; Weinhold et al., 1989) that CD4 cross-linking may have a role in AIDS-related immunosuppression.

The wt31/Leu4 binding sites on PBL may be heterogeneous, given that less wt31 bind than Leu4 upon saturation (~50% in PBS at 0°C, or ~30% in complete medium at 37°C, with the calculation based on the labeling ratios for these mAbs and also verified by indirect staining). Therefore, it is possible that wt31 recognizes a subpopulation of the CD3 ϵ chains, whereas Leu4 may bind to all ϵ chains. If those Leu4 binding sites not accessible to wt31 are not intimately associated with CD4, the overall CD4-CD3 distance calculated by pFRET will appear longer (see, e.g., experiments 10–12). As there are more TCR/CD3 complexes than CD4s (~2×, data not shown), there will be no donors without acceptors upon complete association in the CD4-to-TCR/CD3 FRET experimental arrangement. Our method measures E on the donor side, making this approach (see experiment 8) sensitive exclusively to changes in CD4-TCR/CD3 intimacy (see Materials and Methods). In cocapping experiments performed on the image analyzer, line scans across different sections of the cells revealed an overlap between the OKT4- and Leu4-labeled structures, the overlap being restricted to certain domains of the membrane, suggesting that the two TCR/CD3 subpopulations were situated in distinct membrane domains (data not shown). Furthermore, it is possible that wt31 binds in a monovalent, but Leu4 in a bivalent fashion, since wt31 tends to dissociate from PBL cells upon washing the cells with complete medium performed at room temperature, in contrast with Leu4 (or Leu3a). It is easily imagined that monovalent binding may be more sensitive to possible steric restraints, imposed e.g., by an Ab binding to CD4. Steric hindrance within the TCR/CD3/CD4 complexes could prevent initiation of cell activation via these complexes. Inappropriate (for stimulation) interaction between Leu3a-engaged CD4 and wt31-bound TCR/CD3 may invoke negative signaling.

The question whether T cell suppression by CD4 cross-linking involves wide spatial sequestration of the Ag or if it is due to more subtle forms of steric hindrance is answered by the data above, directly and in an essentially nonperturbing experimental situation. The pFRET technique, probably the most sensitive method developed so far, allowed us to measure intermolecular distances on the surface of human PBL. Surprisingly, cross-linked CD4 stays in the molecular vicinity of TCR, challenging the sequestration hypothesis, visualized as a wide spatial separation of the Ags involved, and supporting the view that an adequate steric apposition of CD4 and the TCR/CD3 complex is required for activation signaling.

Various modifications of our earlier technique (Szabó et al., 1992a, b, 1993) have contributed to the accuracy of our pFRET measurements. Flow-sorting served to increase the efficiency of our measurements (approximately every fourth PBL is expected to be CD4-positive) and helped decrease the biological variation of D/A ratio. Recording FL2 intensity enabled us to analyze our data on FL2/FL1 dot plots (scattergrams) created in the worksheet program. The FL1 decay times could be compared with the relative D/A labeling ratio of the individual cells in a manner similar to a flow-cytometric dot plot (Fig. 3), providing information on conspicuous population heterogeneities. The normalization protocol introduced here enabled us to interpret changes of the energy transfer efficiency (as observed by this D-sided FRET method) in terms of topological changes. It must also be emphasized that the labeled antibodies were applied in relatively low doses, as part of the stimulation experiments, in culture conditions; therefore, the observed topology is assumed to be biologically relevant.

We appreciate valuable comments received from Dr. Janos Szollosi (Debrecen, Hungary) regarding our normalization protocol. We thank Drs. E. Patzer and B. Fendly (Genentech, Inc., South San Francisco, CA) for recombinant gp120 and the anti-gp120 mAb. The reagent Sim.4 was obtained from Dr. James Hildreth through the AIDS Research and Reference Reagent Program, Division of AIDS, NIAID, National Institutes of Health. This work was supported by the U.S.-Hungarian Science and Technology Joint Fund in cooperation with Department of Biophysics, University Medical School of Debrecen, and Division of Research and Testing, Food and Drug Administration under Project JFNO.127 and by OTKA grant 1494 (Hungary).

REFERENCES

Abraham, N., M. C. Miceli, J. R. Parnes and A. Veillette. 1991. Enhancement of T-cell responsiveness by the lymphocyte-specific tyrosine protein kinase p56lck. *Nature.* 350:62–66.

Banda, N. K., J. Bernier, D. K. Kurahara, R. Kurrle, N. Haigwood, R.-P. Sekaly, and T. H. Finkel. 1992. Crosslinking CD4 by human immunodeficiency virus gp120 primes T cells for activation-induced apoptosis. *J. Exp. Med.* 176:1099–1106.

Bank, I., and L. Chess. 1985. Perturbation of the T4 molecule transmits a negative signal to T cells. *J. Exp. Med.* 162:1294–1303.

Burgess, K. E., A. D. Odysseos, C. Zalvan, B. J. Druker, P. Anderson, S. F. Schlossman, and C. E. Rudd. 1991. Biochemical identification of a direct physical interaction between the CD4p56^{lck} and T_i(TCR)/CD3 complexes. *Eur. J. Immunol.* 21:1663–1668.

Collins T. L., S. Uniyal, J. Shin, J. L. Strominger, R. S. Mittler, and S. J. Burakoff. 1992. p56^{lck} association with CD4 is required for the interaction between CD4 and the TCR/CD3 complex and for optimal antigen stimulation. *J. Immunol.* 148:2159–2162.

Dianzani U., A. Shaw, B. K. al-Ramadi, R. T. Kubo, C. A. Janeway Jr. 1992. Physical association of CD4 with the T cell receptor. *J. Immunol.* 148: 678–688.

Gallagher, P., B. Fazekas de St. Groth, and J. F. A. P. Miller. 1989. CD4 and CD8 molecules can physically associate with the same T-cell receptor. *Proc. Natl. Acad. Sci. USA.* 86:10044–10048.

Glaichenhaus, N., N. Shastri, D. R. Littman, and J. M. Turner. 1991. Requirement for association of p56^{lck} with CD4 in antigen-specific signal transduction in T cells. *Cell.* 64:511–520.

Haque S., K. Saizawa, J. Rojo, and C. A. Janeway Jr. 1987. The influence of valence on the functional activities of monoclonal anti-L3T4 antibodies. *J. Immunol.* 139:3207–3212.

Haughn, L. L., S. Gratton, L. Caron, R.-P. Sekaly, A. Veillette, M. H. Julius. 1992. Association of tyrosine kinase p56^{lck} with CD4 inhibits the induction of growth through the alpha beta T-cell receptor. *Nature.* 358:328–331.

Janeway, C. A. Jr. 1989. The role of CD4 in T-cell activation: accessory molecule or co-receptor? *Immunol. Today.* 10:234–238.

Jovin T. M., and D. J. Arndt-Jovin. 1989. Cell Structure and Function by Microspectrofluorimetry. E. Kohen, J. S. Ploem, and J. G. Hirschberg, editors. Academic Press, Orlando, FL. 99–117.

Julius, M., C. R. Maroun, and L. Haughn. 1993. Distinct roles for CD4 and CD8 as co-receptors in antigen signaling. *Immunol. Today.* 14:177–183.

Kupfer A., S. J. Singer, C. A. Janeway Jr., and S. L. Swain. 1987. Coclustering of CD4 (L3T4) molecule with the T-cell receptor is induced by specific direct interaction of helper T cells and antigen-presenting cells. *Proc. Natl. Acad. Sci. USA.* 84:5888–5892.

Langedijk, J. P. M., W. C. Puijk, W.P. van Hoorn, and R. H. Meloen. 1993. Location of CD4 dimerization site explains critical role of CDR3-like region in HIV-1 infection and T-cell activation and implies a model for complex of coreceptor-MHC. *J. Biol. Chem.* 268:16875–16878.

Luo, K. and B. M. Sefton. 1990. Cross-linking of T-cell surface molecules CD4 and CD8 stimulates phosphorylation of the lck tyrosine kinase at the autophosphorylation site. *Mol. Cell. Biol.* 10:5305–5313.

McDonnell, J. M., K. J. Blank, P. E. Rao, and B. A. Jameson. 1992. Direct involvement of the CDR3-like domain of CD4 in T helper cell activation. *J. Immunol.* 149:1626–1630.

Mittler R. S., S. J. Goldman, G. L. Spitalny, and S. J. Burakoff. 1989. T-cell receptor-CD4 physical association in a murine T-cell hybridoma: induction by antigen receptor ligation. *Proc. Natl. Acad. Sci. USA.* 86:8531–8535.

Mittler, R. S., and M. K. Hoffmann. 1989. Synergism between HIV gp120 and gp120-specific antibody in blocking human T cell activation. *Science.* 245:1380–1382.

Mittler, R. S., B. M. Rankin, and P. A. Kiener. 1991. Physical associations between CD45 and CD4 or CD8 occur as late activation events in antigen receptor-stimulated human T cells. *J. Immunol.* 147:3434–3440.

Nel, A. E., S. Pollack, G. Landreth, J. A. Ledbetter, L. Hultin, K. Williams, R. Katz, and B. Akerley. 1990. CD3-mediated activation of MAP-2 kinase can be modified by ligation of the CD4 receptor. *J. Immunol.* 145: 971–979.

Newell, M. K., L. J. Haughn, C. R. Maroun, and M. H. Julius. 1990. Death of mature T cells by separate ligation of CD4 and the T-cell receptor for antigen. *Nature.* 347:286–289.

Rojo, J. M., and C. A. Janeway Jr. 1988. The biologic activity of anti-T cell receptor V region monoclonal antibodies is determined by the epitope recognized. *J. Immunol.* 140:1081–1088.

Rojo J. M., K. Saizawa, and C. A. Janeway Jr. 1989. Physical association of CD4 and T-cell receptor can be induced by anti-T-cell receptor antibodies. *Proc. Natl. Acad. Sci. USA.* 86:3311–3315.

Rudd E. E, J. M. Trevillyan, J. D. Dasgupta, L. L. Wong, and Schlossman. 1988. The CD4 receptor is complexed in detergent lysates to a protein-tyrosine kinase (pp58) from human T lymphocytes. *Proc. Natl. Acad. Sci. USA.* 85:5190–5194.

Saizawa K., J. Rojo, and C. A. Janeway Jr. 1987. Evidence for a physical association of CD4 and the CD3:alpha:beta T-cell receptor. *Nature.* 328: 260–263.

Salmeron, A., F. Sanchez-Madrid, M. A. Ursa, M. Fresno, and B. Alarcon. 1991. A conformational epitope expressed upon association of CD3-epsilon with either CD3-delta or CD3-gamma is the main target for recognition by anti-CD3 monoclonal antibodies. *J. Immunol.* 147: 3047–3052.

Sattentau, Q. J., A. G. Dalgleish, R. A. Weiss, P. C. L. Beverley. 1986. Epitopes of the CD4 antigen and HIV infection. *Science.* 234:1120–1123.

Straus D. B., and A. Weiss. 1992. Genetic evidence for the involvement of the lck tyrosine kinase in signal transduction through the T cell antigen receptor. *Cell.* 70:585–593.

Suzuki, S., J. Kupsch, K. Eichmann, and M. K. Saizawa. 1992. Biochemical evidence of the physical association of the majority of sigma chains with the accessory/co-receptor molecules CD4 and CD8 on nonactivated T lymphocytes. *Eur. J. Immunol.* 22:2475–2479.

Szabó, G. Jr., P. S. Pine, J. L. Weaver, M. Kasari, and A. Aszalos. 1992a. Epitope mapping by photobleaching fluorescence resonance energy transfer measurements using a laser scanning microscope system. *Biophys. J.* 61:661–669.

Szabó, G. Jr., P. S. Pine, J. L. Weaver, P. E. Rao, and A. Aszalos. 1992b. CD4 changes conformation upon ligand binding. *J. Immunol.* 149: 3596–3604.

Szabó, G. Jr., J. L. Weaver, P. S. Pine, and A. Aszalos. 1993. Specific disengagement of cell-bound αLAM-1 antibodies by aurintricarboxylic acid. *Mol. Immunol.* 30:1689–1694.

Veillette A., M. A. Bookman, E. M. Horak, and J. B. Bolen. 1988. The CD4 and CD8 T cell surface antigens are associated with the internal membrane tyrosine-protein kinase p56lck. *Cell.* 55:301–308.

Weinhold K. J., H. K. Lyerly, S. D. Stanley, A. A. Austin, T. J. Matthews, and D. P. Bolognesi. 1989. HIV-1 gp120-mediated immune suppression and lymphocyte destruction in the absence of viral infection. *J. Immunol.* 142:3091–3097.

Xu, H., and D. R. Littman. 1993. A kinase-independent function of Lck in potentiating antigen-specific T cell activation. *Cell.* 74:633–643.